**PHYSICS AND CHEMISTRY OF SOLID STATE**
V. 24, No. 1 (2023) pp. 17-22
*Section: Physics*

**DOI: 10.15330/pcss.24.1.17-22**

*Vasyl Stefanyk Precarpathian National University*

**ФІЗИКА І ХІМІЯ ТВЕРДОГО ТІЛА**
**Т. 24, № 1 (2023) С. 17-22**
*Фізико-математичні науки*

UDC: 621.315.592 ISSN 1729-4428

M.Ya. Rudysh[1,2,3], O.V. Smitiukh[1], G.L. Myronchuk[1], S.M. Ponedelnyk[1], O.V. Marchuk[1]

# Band Structure Calculation and Optical Properties of $Ag_3AsS_3$ Crystals

[1]*Lesya Ukrainka Volyn National University, Lutsk, Ukraine, myronchuk.halyna@vnu.edu.ua*
[2]*J. Dlugosz University in Częstochowa, Czestochowa, Poland*
[3]*Ivan Franko National University of Lviv, Lviv, Ukraine*

In the study, band structure calculation in the points of high symmetry of the first Brillouin zone and alongside the lines that connect them has been derived by using CASTEP programs in which the pseudopotential method with the basis in the form of plane-waves is realized. The calculated value of the lattice parameters using GGA functional is well correlated with experimental data. According to the band diagram that was built for the $Ag_3AsS_3$ crystal using GGA method, band gap has an indirect type. The calculated value of the band gap is $E_g$ = 1.22 eV. The experimental value of the band gap obtained by Tauc's method is $E_g^{ind}$ = 2.01 eV, $E_g^{dir}$ = 2.17 eV. Full and partial density of *N*(*E*) states for contributions of separate atoms has been calculated. As a result, the top of the valence band is formed by 3*p*-states of S atoms and the bottom of the conduction band is formed by 5*s*-states of Ag atoms and 3*p*-states of S atoms.

**Keywords:** $Ag_3AsS_3$, band structure, density functional theory, optical spectrum.

*Received 14 September 2022; Accepted 16 February 2023.*

## Introduction

The $Ag_3AsS_3$ (proustite) crystals are interesting due to their physical properties and potential of technical application [1–5]. They have been investigating as prospective materials for electronics because they are piezoelectrics, pyroelectrics, as well as thermal and photosensetive semiconductors. The $Ag_3AsS_3$ crystal is characterized by a dark conductivity of hole mechanism and high resistivity [6-9]. According to the requirements that are for non-linear optical materials in IR region, $Ag_3AsS_3$is an acentric single crystal with large non-linear-optical coefficients $d_{31}$ = 10.4 pm/V, that is approximately 1.1 times larger than a commercially used AGS ($d_{31}$ = 30 times $d_{36}$ in KDP, $d_{22}$ = 50 times $d_{36}$ in KDP), high refractive index (~3.0), large negative birefringence in the IR region of the spectrum and high transparency in a wide range (0.6-13μm except a strong absorption band at 1600 $cm^{-1}$) [3-5].

In order to understand all processes and phenomena better, we need to have more information at crystal structure of materials and their change under the influence of external fields. The considerable importance has data about electronic band structure with which certain properties can be associated. This study is devoted to the band structure calculation of the $Ag_3AsS_3$ crystals by *ab initio* methods.

## I. Calculation method

The calculations have been carried out by using Cambridge Serial Total Energy Package (CASTEP) program [10] based on the density functional theory (DFT) [11]. The program implements the pseudopotential method with a basis in the form of plane-waves. All electrons of atoms were divided to the two groups: valence electrons (determine the main properties) and core electrons (inert). Ag $4d^{10}$ $5s^1$, S $3s^2$ $3p^4$, As $4s^2$ $4p^3$ electronic configurations have been used as valence electrons. The core electrons together with nuclear charge were counted in pseudopotential. The ultrasoft Vanderbilt

pseudopotential [12] was used in the calculations which, in comparison with the norm-conserving pseudo potential, require a smaller number of plane-waves (smaller basis). The exchange-correlation interaction was considered as a generalized gradient approximation (GGA) in the form of Perdew-Burke-Ernzerhoff (PBE) parametrization [13]. The cut-off energy of plane waves was chosen to be equal to 350 eV. Integration was carried out on a 3×3×3 k-mesh chosen according to the Monkhorst-Pack scheme [14]. The Kohn-Sham equation was solved self-consistently. This procedure was carried out until the energy difference of the system in successive steps reached a value of $24 \times 10^{-7}$ eV. For optimization of the crystal structure Broyden–Fletcher–Goldfarb–Shanno (BFGS) algorithm was used [15]. The structure was optimized until the forces acting on each ion were greater than 0.02 eV/Å and the total energy of the system coincided with an accuracy of $5\times10^{-6}$ eV/atom, the maximum pressure was 0.02 GPa, and the maximum ion displacement was $5.0\times10^{-4}$ Å.

Band structure calculations were performed for the high-symmetry points of the first Brillouin zone and along the lines connecting them. For the $Ag_3AsS_3$ crystal, the band structure calculations have been performed along the Brillouin zone in the direction Γ→A→H→K→Γ→M→L→H.

## II. Results and discussion

### 2.1. Crystal structure

The unit cell of the pure $Ag_3AsS_3$ crystal consists of 42 ions that are formed by three types of atoms. The crystal belongs to the trigonal symmetry (hexagonal scalenohedral -3*m* crystal class) and has a space group $C_{3v}^6$ (space group No.161) [16].

The structural parameters of investigating compound are presented in Table 1 and 2. As can be seen from Table 1, calculated (by using GGA functional method) and measured values [16] for the lattice parameters correlate well. The general view of the unit cell is presented in Fig. 1.

### 2.2. Electronic band structure of the $Ag_3AsS_3$ crystal

Band structure calculation that determines certain properties of material have been carried out by using the GGA method. Band diagram *E*(k) was built along the directions that connect the special points of the first Brillouin zone (Γ→A→H→K→Γ→M→L→H). The view of the first Brillouin zone of the investigating crystal is presented in Fig.2.

Band diagram that was built for the $Ag_3AsS_3$ crystal is presented in Fig.3 (a). As can be seen in Fig.3 (a), the $Ag_3AsS_3$ crystal has an indirect band gap.

The top of the valence band is located in the center of Brillouin zone (point Γ(0; 0; 0)). The bottom of the conduction band is formed by two broad sub bands (0 – – 6 eV and 1.2 – 8 eV). The lower levels of the valence band formed by narrow sub bands nearby 10, 13 and 14.5 eV. Previously the electronic band structure of the $Ag_3AsS_3$ crystal had been calculated within the tight-binding method with the correction with experimental data [17]. The general view of *E*(k) in the work [17] depicts peculiarities of the band diagram that we calculated using DFT. The calculated value of the band gap using GGA method is $E_g$ = 1.22 eV. At the same time, the experimental value of the band gap calculated by Tauc's method (Fig.4) is $E_g^{ind}$ = 2.01 eV and $E_g^{dir}$ = 2.17 eV. These results are consistent with the works [1, 18].

**Table 1.**

The experimental structure parameters of the$Ag_3AsS_3$ crystal and theoretically calculated ones (optimized with GGA functional).

| Parameter | GGA | Exp.[16] |
|---|---|---|
| $a = b$(Å) | 10.783 | 10.813 |
| $c$ (Å) | 9.456 | 8.691 |
| $\alpha$ (°) | 90 | 90 |
| $\beta$(°) | 90 | 90 |
| γ (°) | 120 | 120 |
| $V$ (Å$^3$) | 952.297 | 880.199 |

**Table 2.**

Fractional atomic coordinates of the $Ag_3AsS_3$ crystal given in the work [16].

| Atom | Site | *x/a* | *y/b* | *z/c* |
|---|---|---|---|---|
| Ag | 18*b* | 0.2483 | 0.2980 | 0.2194 |
| As | 6*a* | 0 | 0 | 0 |
| S | 18*b* | 0.2129 | 0.0926 | 0.3743 |

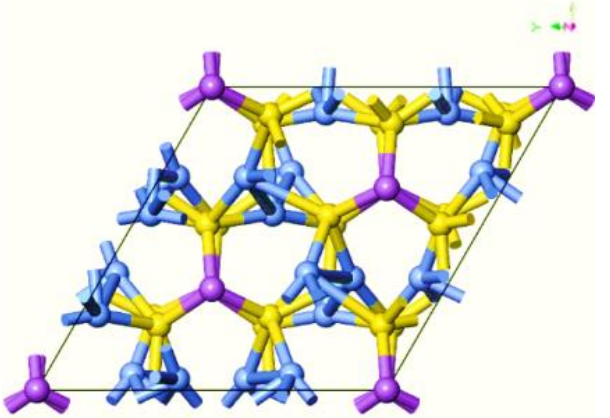

**Fig.1**. The projection of the unit cell of the $Ag_3AsS_3$ crystal on the *xy* plane.

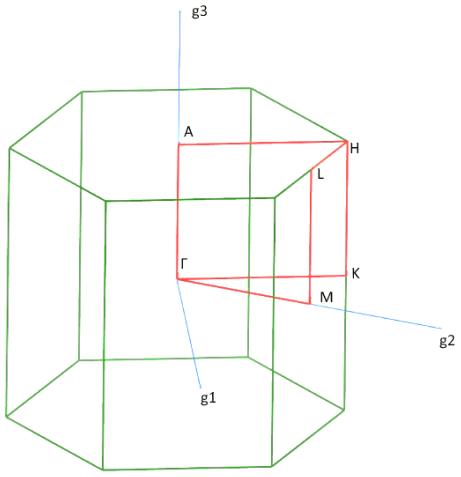


**Fig.2.** The view of the first Brillouin zone of the $Ag_3AsS_3$ investigating crystal: Γ(0;0;0); A(0;0;1/2); H(–0.333; 0.667; 0); K(–0.333; 0.667; 0); Γ(0; 0; 0); M(0;1/2; 0); L(0; 1/2; 1/2); H(–0.333; 0.667; 1/2) – points of high symmetry, $g_1$, $g_2$, and $g_3$ – directions of axes in the reciprocal lattice.

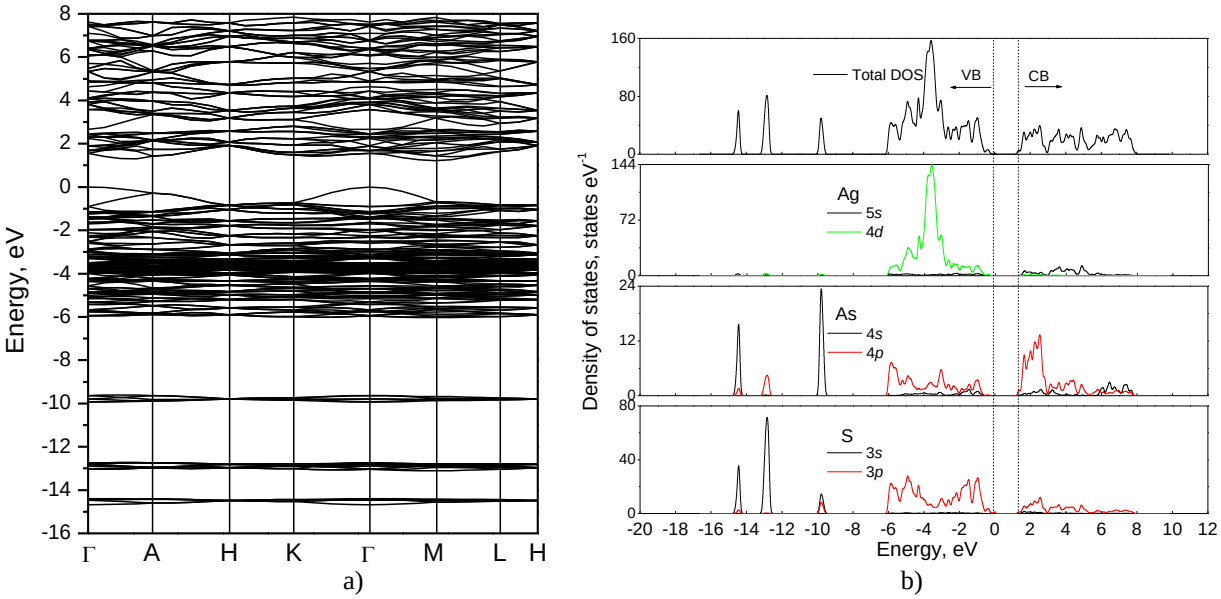


**Fig.3.** The electronic structure (a) and density of states (b) of the $Ag_3AsS_3$ crystal obtained with using GGA functional.

For detailed study of origin of energy levels, we calculated total and partial density of states (PDOS) $N(E)$ for contributions of individual atoms (Fig.3(b)). As can been seen in Fig.3(b), the top of the valence band is formed by 3-*p*states of S atoms. They together with 4*p*-states of As atoms form the broad band from 0 to –6 eV. The intensive peak around –5 eV corresponds to 4*d*-states. The valence states around –10 eV are formed by core As 4*s*-electrons. At energy –13 eV the localized level is formed by 3*s*-states of sulfur with a minor contribution of As 4*p*-electrons. At energy –14.5 eV the narrow peak is formed by 3*s* and 4*s*-states of As and S, respectively. The bottom of conduction band is formed by 5*s*-states of Ag and 3*p*-states of S. It worth noting that the origin of electronic levels that create a band gap is correlated to the results obtained in the work [17].

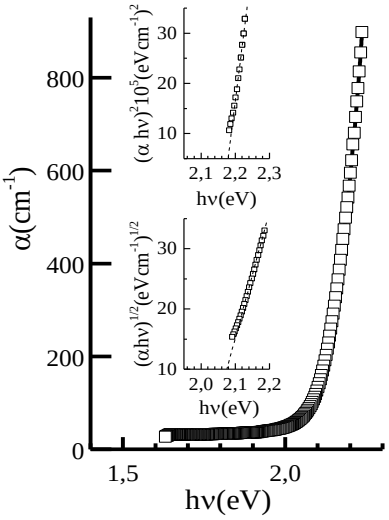


**Fig. 4.** Spectral dependence of the absorption coefficient of $Ag_3AsS_3$.

### 2.3. Optical properties

The results of band structure calculation may be used for an analysis of optical properties of materials. It is well-known that optical properties of materials are determined with dielectric function ε that depends on frequency ε(ω) (energy). The function is complex and consist of real $\varepsilon_1(\omega)$ and imaginary $\varepsilon_2(\omega)$ parts. For the $Ag_3AsS_3$ crystal optical properties are obtained from the frequency dependence of the complex dielectric function $\varepsilon(\omega) = \varepsilon_1(\omega) + i\varepsilon_2(\omega)$, where $i = \sqrt{-1}$. It is also known that the real part of dielectric function explains refractive properties and is related to the refractive index. The imaginary part $\varepsilon_2(\omega)$ explains processes of light absorption in the material and associated with transitions of electrons to higher energy levels during light absorption [19]. The frequency dependence of the imaginary part of the dielectric function $\varepsilon_2(\omega)$ is calculated using equation (1) by integrating in k-space the elements of the dipole matrix operator between the filled states in the valence band and the empty states of the conducting band levels

$$\varepsilon_2(\omega) = \frac{2\pi e^2}{\Omega\varepsilon_0}\sum_{k,v,c}|\langle\psi_k^c|u\boldsymbol{r}|\psi_k^v\rangle|^2\delta(E_k^c - E_k^v - E), \quad (1)$$

where $E$ is energy; $u$ the vector of polarization of incident beam; $\psi_k^c$ and $\psi_k^v$ are a wave functions of the conduction band and valence band in $k$-space, respectively; $\Omega$ is volume of a unit cell; $e$ is the electron charge; $\varepsilon_0$ the dielectric constant for vacuum; $\mathbf{r}$ is electron position operator.

The real $\varepsilon_1(\omega)$ can be obtained from an imaginary dielectric function. For this, the well-known Kamers-Kronig relation is used. The relation connects the spectral dependence of the real and imaginary parts of the dielectric function [20]:

$$\varepsilon_1(\omega) = 1 + \frac{2}{\pi}\int_0^\infty \frac{\varepsilon_2(\omega')\omega'\,d\omega'}{\omega'^2 - \omega^2}. \quad (2)$$

The spectrum of the real $\varepsilon_1(\omega)$ and imaginary $\varepsilon_2(\omega)$ parts was calculated using GGA functional. The frequency dependence of $\varepsilon_1$ and $\varepsilon_2$ calculated for the light wave polarization directions $E||Z$ and $E\perp Z$ are shown in Fig.5. As shown in figure, the dielectric function is characterized

by significant anisotropy, which is determined by the difference in the positions of the bands and their intensities. Also, for the comparison of dielectric function Fig.5 contain its experimentally obtained real and imaginary part reported in [17]. The theoretical dielectric functions are consistent with the experimental. Insignificant deviations can be related to not taking into account indirect transitions. According to group theoretical analysis performed within the dipole approximation [21] the allowed inter band transitions in the center of first Brillouin zone between electronic states (without spin consideration) are following:$\Gamma_1 \rightarrow \Gamma_3$, $\Gamma_3 \rightarrow \Gamma_1$, $\Gamma_2 \rightarrow \Gamma_3$, $\Gamma_3 \rightarrow \Gamma_2$– for $E \perp Z$, and $\Gamma_1 \rightarrow \Gamma_1$, $\Gamma_2 \rightarrow \Gamma_2$, $\Gamma_3 \rightarrow \Gamma_3$ – for $E \| Z$. As expected, the dielectric function for $E \perp Z$ polarization of light the is more instance than for $E \| Z$ polarization. This is confirmed by the larger amount of allowed transitions in Γ point.

From spectral dependence of real and imaginary parts of dielectric functions we can obtain other optical properties also, for instance, a refractive index $n(\omega)$, the coefficient of extinction $k(\omega)$ which are related to each other as follows $N = n + ik$.

In the work, $n$ and $k$ are calculated using following formulas [22]:

$$n = \sqrt{\frac{(\varepsilon_1^2+\varepsilon_2^2)^{1/2}+\varepsilon_1}{2}}, \quad k = \sqrt{\frac{(\varepsilon_1^2+\varepsilon_2^2)^{1/2}-\varepsilon_1}{2}}. \qquad (3)$$

Frequency dependence of refractive index $n_i$ and the extinction coefficient $k_i$ of the $Ag_3AsS_3$ crystal is presented in Fig.6.

Other parameter that is related to the dielectric function is the absorption coefficient of material α. It is obtained from expression:

$$\alpha = \frac{2k\omega}{c}, \qquad (4)$$

and it indicates the part of lost energy loss due to the passage of the wave through the material.

It can be seen from the figure that the calculated dependence of the absorption coefficient of the crystal is characterized by an increase in α with increasing photon energy, reaching a maximum at an energy of approximately 8.5 eV, followed by a rapid decrease. Also, it is worth noting that the studied crystal has a large value of the absorption coefficient α, which lies within the range of 1-3 $\times 10^5$ $cm^{-1}$. A similar high value was previously obtained for other crystals of group I-III-$VI_2$, which is also of the order of $10^5$ $cm^{-1}$ [23,24].

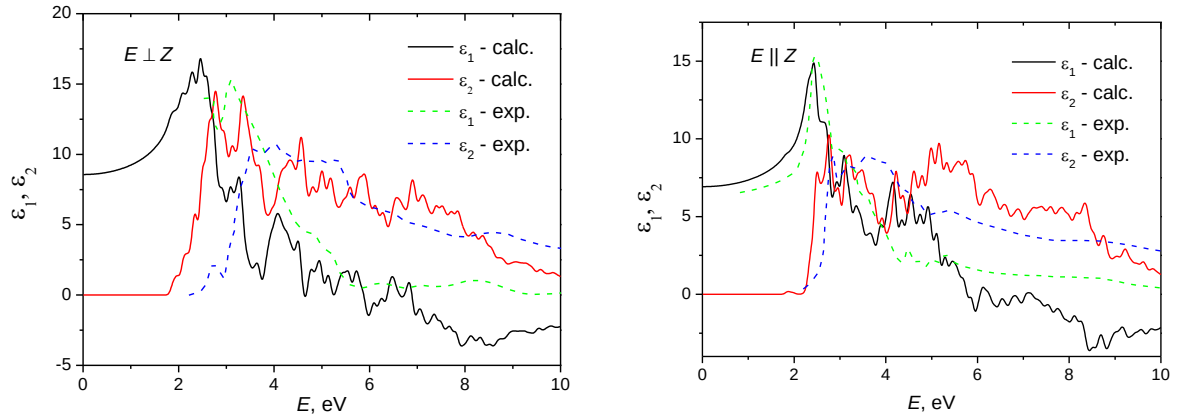


a) b)

**Fig.5.** The spectral dependence of the real and imaginary parts of the dielectric function are calculated using the GGA functional for the directions of light polarization (a) $E \perp Z$ and (b) $E \| Z$ (experimental data taken from work [16]).

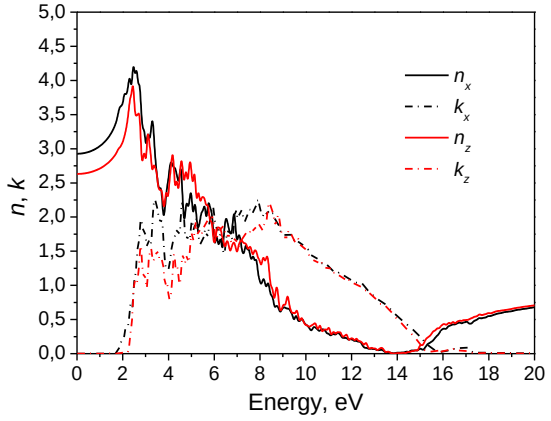


**Fig.6.** Spectral dependence of the refractive index $n$ and the extinction coefficient $k$ of the $Ag_3AsS_3$ crystal calculated using the GGA functional.

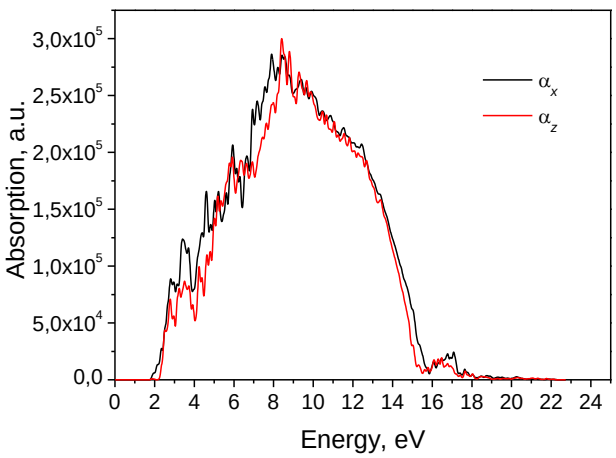


**Fig.7.** Spectral dependence of absorption coefficient $\alpha$ of the $Ag_3AsS_3$ crystal for directions $E \perp Z$ and $E \| Z$ calculated using the GGA functional.

## Conclusions

In the study, the band structure calculation in the points of high symmetry of the first Brillouin zone and along the lines connecting them have been prepared using CASTEP program based on pseudo potential method with basis in the form of plane waves. The calculated and measured parameters of the lattice are correlated well. According to the band structure of the $Ag_3AsS_3$ crystal that was built using GGA functional method, the band gap is indirect. The calculated value of band gap is $E_g$ = 1.22 eV. The experimental value of band gap estimated by Tauc's method is $E_g^{ind}$=2.01 eV and $E_g^{dir}$=2.17 eV, respectively. The full and partial density of states $N(E)$ for contributions of individual atoms have been calculated. As a result, the top of the valence band formed by 3*p*-states of S and the bottom of the conduction band formed by 5*s*-states of silver and 3*p*-states of sulfur. A spectral dependences of the optical function has been calculated. Shown a good agreement with the experimental data.

**Acknowledgments**

*This work was supported by the PRELUDIUM 15 program of Polish National Science Center (Grant No. 2018/29/N/ST3/02901).*

***Rudysh M.Ya.*** – Candidate of Physical and Mathematical Sciences, senior researcher of the Department of General Physics of Ivan Franko Lviv National University;
***Smitiukh O.V.*** – candidate of chemical sciences, senior laboratory technician of the Department of Chemistry and Technologies, Faculty of Chemistry, Ecology and Pharmacy of Lesya Ukrainka Volyn National University;
***Myronchuk G.L.*** – doctor of physical and mathematical sciences, professor, director of the educational-scientific physical-technological institute of Volyn National University named after Lesya Ukrainka;
***Ponedelnyk S.M.*** – graduate student of Volyn National University named after Lesya Ukrainka;
***Marchuk O.V.*** – candidate of chemical sciences, docent of the Department of Chemistry and Technologies, Faculty of Chemistry, Ecology and Pharmacy of Lesya Ukrainka Volyn National University.

[1] V.V. Zalamai, A.V. Tiron, I.G. Stamov, S.I. Beril, *Wavelength modulation optical spectra of $Ag_3AsS_3$ crystals in the energy gap*, Optical Materials, 129, 112560 (2022); https://doi.org/10.1016/j.optmat.2022.112560.
[2] H. Lin, W.B. Wei, H. Chen, X.T. Wu, Q.L. Zhu, *Rational design of infrared nonlinear optical chalcogenides by chemical substitution*, Coord. Chem. Rev. 406, 213150 (2020); https://doi.org/10.1016/j.ccr.2019.213150.
[3] Kui Wu, Shilie Pa,. *A review on structure-performance relationship toward the optimal design of infrared nonlinear optical materials with balanced performances*, Coord. Chem. Rev. 377, 191 (2018); https://doi.org/10.1016/j.ccr.2018.09.002.
[4] Fei Liang, Lei Kang, Zheshuai Lin, and Yicheng Wu, *Mid-Infrared Nonlinear Optical Materials Based on Metal Chalcogenides: Structure–Property Relationship Cryst*, Growth Des., 17(4), 2254 (2017); https://doi.org/10.1021/acs.cgd.7b00214.
[5] A. Abudurusuli, J. Li, S. Pan, *A review on the recently developed promising infrared nonlinear optical materials*, Dalt. Trans. 50, 3155 (2021); https://doi.org/10.1039/D1DT00054C.
[6] V. Kavaliukė, T. Šalkus, A. Kežionis, M.M. Pop, I.P. Studenyak, *$Ag_3AsS_3$-$As_2S_3$ composite: Detailed impedance spectroscopy study*, Solid State Ionics, 383, 115971 (2022); https://doi.org/10.1016/j.ssi.2022.115971.
[7] V. S. Bilanych, R. Yu. Buchuk, K. V. Skubenych, I. I. Makauz, I. P. Studeniak, *Relaxation Processes in Silver Containing Superionic Composites in the System $Ag_3AsS_3$-$As_2S_3$*, Physics and Chemistry of Solid State, 13 (3), 625 (2012). Rezhym dostupu: http://nbuv.gov.ua/UJRN/PhKhTT_2012_13_3_12.(In Ukrainian)
[8] V. A. Bordovsky, N. Yu. Gunia, R. A. Castro, *High-frequency dielectric study of proustite crystals $Ag_3AsS_3$*, Journal of Physics: Conference Series, 572, 012019 (2014); https://doi.org/10.1088/1742-6596/572/1/012019.
[9] O.V. Smitiukh, O.V. Marchuk, Y.M. Kogut, V.O. Yukhymchuk, N.V. Mazur, G.L.Myronchuk, S.M. Ponedelnyk, O.I. Cherniushok, T.O. Parashchuk, O.Y. Khyzhun, K.T. Wojciechowski, A.O. Fedorchuk, *Effect of rare-earth doping on the structural and optical properties of the $Ag_3AsS_3$ crystals*, Optical and Quantum Electronics, 54:4, 224 (2022); https://doi.org/10.1007/s11082-022-03542-w.
[10] S.J. Clark, M.D. Segall, C.J. Pickard, P.J. Hasnip, M.J. Probert, K. Refson, M.C. Payne, *First principles methods using CASTEP*, Z. Kristallogr, 220, 567 (2005); https://doi.org/10.1524/zkri.220.5.567.65075.
[11] P. Hohenberg, W. Kohn, *Inhomogeneous Electron Gas*, Phys. Rev. 136, B864 (1964); https://doi.org/10.1103/PhysRev.136.B864.
[12] D. Vanderbilt, *Soft self-consistent pseudopotentials in a generalized eigenvalue formalism*, Phys. Rev. B. 41, 7892 (1990); https://doi.org/10.1103/PhysRevB.41.7892.
[13] J.P. Perdew, A. Zunger, *Self-interaction correction to density-functional approximations for many-electron systems*, Phys. Rev. B 23, 5048 (1981); https://doi.org/10.1103/PhysRevB.23.5048.
[14] H.J. Monkhorst and J.D. Pack, *Special points for Brillouin-zone integrations*, Phys. Rev. B, 13, 5188 (1976); https://doi.org/10.1103/PhysRevB.13.5188.
[15] B.G. Pfrommer, M. Côté, S.G. Louie, M.L. Cohen, *Relaxation of Crystals with the Quasi-Newton Method*, Journal of Computational Physics, 131, 233 (1997); https://doi.org/10.1006/jcph.1996.5612.
[16] A. Gagor, A. Pawłowski, A. Pietraszko, *Silver transfer in proustite $Ag_3AsS_3$ at high temperatures: Conductivity and single-crystal X-ray studies*, J. Solid State Chem. 182(3), 451 (2009); DOI:10.1016/j.jssc.2008.11.005.

[17] Ya.O. Dovgii, I.V. Kityk, *Band Structure and Nonlinear Optical Susceptibilities of Proustite ($Ag_3AsS_3$)*, Phys. Stat. Sol. (b), 166, 395 (1991); https://doi.org/10.1002/pssb.2221660208.
[18] Marvin J. Weber, Handbuk of optical materials (CRC Press, 2002).
[19] Mark Fox, Optical properties of solids (Oxford University Press, Oxford (2001)).
[20] M. Dressel, B. Gompf, D. Faltermeier, A.K. Tripathi, J. Pflaum and M. Schubert, *Kramers-Kronig-consistent optical functions of anisotropic crystals: generalized spectroscopic ellipsometry on pentacene*, Opt.Express 16. 19770- (2008); https://doi.org/10.1364/OE.16.019770.
[21] Ya.O. Dovhyj I.V. Kityk, The electronic structure and optics of the nonlinear crystals. 176 p. (Monograph. – Lviv. Svit publisher. 1996).
[22] Sonali Saha, T.P. Sinha and Abhijiti Mookerjee, *Electronic structure, chemical bonding, and optical properties of paraelectric $BaTiO_3$*, Phys. Rev. B 62, 8828 (2000); https://doi.org/10.1103/PhysRevB.62.8828.
[23] M.Ya. Rudysh, P.A. Shchepanskyi, A.O. Fedorchuk, M.G. Brik, V.Yo. Stadnyk, G.L. Myronchuk, E.A. Kotomin, M. Piasecki, *Impact of anionic system modification on the desired properties for $CuGa(S_{1-x}Se_x)_2$ solid solutions, Computational Materials Science*, 196, 110553 (2021); https://doi.org/10.1016/j.commatsci.2021.110553.
[24] M.Ya. Rudysh, M. Piasecki, G.L. Myronchuk, P.A. Shchepanskyi, V.Yo. Stadnyk, O.R. Onufriv, M.G. Brik, $AgGaTe_2$ – The thermoelectric and solar cell material: Structure, electronic, optical, elastic and vibrational features, Infrared Physics and Technology, 111, 103476 (2020); https://doi.org/10.1016/j.infrared.2020.103476.

М.Я. Рудиш[1,2,3], О.В.Смітюх[1], Г.Л. Мирончук[1], С.М.Понедельник[1], О.В. Марчук[1]

# Зонна структура та оптичні властивості кристалів $Ag_3AsS_3$

[1]*Волинський національний університет імені Лесі Українки, Луцьк, Україна, myronchuk.halyna@vnu.edu.ua*
[2]*Гуманітарно-природничий університет імені Яна Длугоша в Ченстохові, Ченстохова, Польща*
[3]*Львівський національний університет імені Івана Франка, Львів, Україна*

У роботі проведено розрахунок зонної структури у точках високої симетрії першої зони Бріллюена і вздовж ліній, що їх з'єднують за допомогою програми CASTEP в якій реалізований псевдо потенціальний метод з базисом у вигляді плоских хвиль. Розраховані значення параметрів ґратки з використанням GGA функціоналів добре узгоджуються з експериментальними даними. Згідно зонної діаграми, побудованої використовуючи GGA метод для кристала $Ag_3AsS_3$, заборонена зона є непрямого типу. Розраховане нами значення ширини забороненої зони становить $E_g$= 1,22 еВ. Експериментальне значення ширини забороненої зони оціненої методом Тауца становить $E_g^{ind}$ = 2,01 еВ, $E_g^{dir}$= 2,17 еВ.

Розраховано повну та парціальну густини станів $N(E)$ для внесків окремих атомів встановлено, що вершина валентної зони утворена 3*p*-станами сірки, а дно зони провідності утворене 5*s*-станами срібла та 3*p*-станами сірки.

**Ключові слова:** $Ag_3AsS_3$, зонна структура, теорія функціонала густини, оптичні спектри.